

# Analytical Solutions for Pore-Fluid Flow Focusing Within Inclined Elliptic Inclusions in Pore-Fluid-Saturated Porous Rocks: Solutions Derived in an Elliptical Coordinate System<sup>1</sup>

Chongbin Zhao,<sup>2,3</sup> B. E. Hobbs,<sup>3</sup> A. Ord,<sup>3</sup> Shenglin Peng,<sup>2</sup>  
Liangming Liu,<sup>2</sup> and H. B. Mühlhaus<sup>3</sup>

---

*Exact analytical solutions have been derived rigorously for the pore-fluid velocity, pore-fluid-flow focusing factor, stream function and excess pore-fluid pressure around and within a buried inclined elliptic inclusion in pore-fluid-saturated porous rocks. The geometric characteristics of the buried inclined elliptic inclusion are represented by the aspect ratio and dip angle of the inclusion, while the hydrodynamic characteristic is represented by the permeability ratio of the elliptic inclusion to its surrounding rock. Since an elliptic inclusion of any aspect ratio can be used to approximately represent geological faults and cracks, the present analytical solutions can be used to investigate the pore-fluid-flow patterns around buried faults and cracks within the crust of the Earth. Therefore, the present analytical solution not only provides a better understanding of the physics behind the pore-fluid-flow focusing problem around and within buried faults and cracks, but also provides a valuable benchmark solution for validating any numerical method in dealing with this kind of pore-fluid-flow focusing problem. The pore-fluid-flow focusing factor of a buried elliptic inclusion is demonstrated to be dependent on the aspect ratio, the permeability ratio and the dip angle.*

---

**KEY WORDS:** theoretical analysis, analytical solution, pore-fluid flow, buried inclined elliptic inclusion.

## INTRODUCTION

Analytical solutions for pore-fluid flow around and within a buried inclined elliptic inclusion in pore-fluid-saturated porous rocks are useful at least for the following two purposes. (1) They can be used to gain some basic understanding of the physics behind the pore-fluid flow pattern around buried faults and

---

<sup>1</sup>Received 10 May 2005; accepted 6 March 2006; Published online: 29 March 2007.

<sup>2</sup>Computational Geosciences Research Centre, Central South University, Changsha, Hunan, China.

<sup>3</sup>CSIRO Division of Exploration and Mining, P. O. Box 1130, Bentley, WA 6102, Australia; e-mail: Chongbin.Zhao@csiro.au

cracks, especially when they are of elliptic geometries. (2) They can be used to validate, directly or indirectly, any numerical method for solving this kind of problem. Although the analytical solutions are available for pore-fluid flow around an elliptic inclusion in a full plane for two extreme situations where an elliptic inclusion is either perfectly permeable or perfectly impermeable (Lamb, 1975; Phillips, 1991), they are not available in other common situations where an elliptic inclusion is neither perfectly permeable nor perfectly impermeable. Note that in the case of a perfectly-permeable elliptic inclusion, the permeability ratio of the elliptic inclusion to its surrounding rock is infinite, while in the case of a perfectly-impermeable elliptic inclusion, the permeability ratio of the elliptic inclusion to its surrounding rock is zero. The permeability ratio of a buried fault or crack to its surrounding rock is usually of a finite value, thus, the major contribution of this paper is to derive exact analytical solutions, which have been hitherto unavailable, for pore-fluid flow around and within an inclined elliptic inclusion of any finite permeability in pore-fluid-saturated porous rocks.

Buried faults and cracks may play an important role in fluid flow in the Earth's upper crust (Zhao and Valliappan, 1994a, 1994b; Jamtveit and Yardley, 1997; Connolly, 1997; Zhao and others, 1999, 2001, 2002). For example, in the field of groundwater engineering, buried faults and cracks can function as pore-fluid flow channels and play a significant role in controlling groundwater flow and contaminant transport so that they can influence both water supply and water quality in a groundwater system. In the field of ore body formation and mineralization, buried faults and cracks can provide favorable flow-focusing environments for the formation and localization of some economic ore deposits within the crust of the Earth. In the field of seismology, buried faults and large cracks can change the site seismic activity through the focused-flow induced rupture and failure processes that are caused by the interaction between material deformation and pore-fluid flow around buried faults and large cracks. Therefore, a better understanding of the pore-fluid flow pattern around buried faults and large cracks within the Earth's crust has become an important research topic in several disciplines of geosciences for many years.

Based on the above considerations, analytical solutions have been derived rigorously for the pore-fluid velocity, pore-fluid-flow focusing factor, stream function and excess pore-fluid pressure around and within an inclined elliptic inclusion, which is a typical representation of a buried fault or crack of elliptic shape in pore-fluid-saturated porous rocks. The derived analytical solutions are fundamentally useful for a better understanding of pore-fluid flow around a buried fault and crack within the crust of the Earth. Some interesting conclusions in relation to the effects of inclined faults and cracks on the pore-fluid-flow focusing phenomenon have been made through this theoretical investigation.

### DERIVATION OF ANALYTICAL SOLUTIONS FOR AN INCLINED ELLIPTIC INCLUSION IN PORE-FLUID SATURATED POROUS ROCKS

Due to mathematical complexities in describing the problem of pore-fluid flow around an inclined elliptic inclusion of any inclined angle, three different coordinate systems are used to mathematically derive the analytical solution for the problem. As shown in Figure 1, these three different coordinate systems are a global Cartesian ( $XY$ ) coordinate system, a local Cartesian ( $xy$ ) coordinate system and a local elliptical  $\xi\eta$  coordinate system respectively. Both the pore-fluid flow in the unperturbed far field and the dip angle of an inclined elliptic inclusion are described in the global  $XY$  coordinate system. The perturbed pore-fluid flow around the inclined elliptic inclusion is described in the local  $xy$  and  $\xi\eta$  coordinate systems. As can be demonstrated later, the use of a local  $\xi\eta$  coordinate system enables boundary conditions between the inclined elliptic inclusion and its surrounding rock to be easily described. If the pore-fluid flow in the unperturbed far field is horizontal, its corresponding components in the local

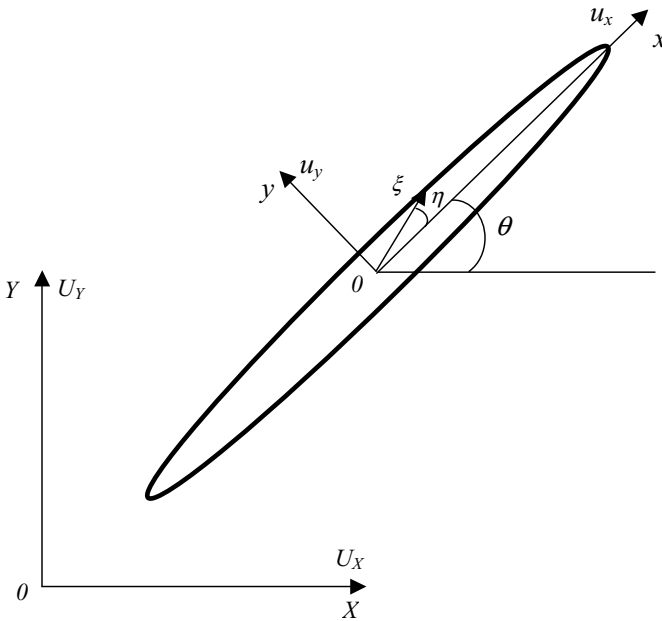


**Figure 1.** Description of an inclined elliptic inclusion in three coordinate systems.

$xy$  coordinate system can be expressed as follows.

$$U_x = U_X \cos \theta, \quad U_y = -U_X \sin \theta \quad (1)$$

where  $U_x$  and  $U_y$  are the pore-fluid velocity components of the far field in the  $x$  and  $y$  directions of the local  $xy$  coordinate system;  $U_X$  is the horizontal pore-fluid velocity component of the far field in the  $X$  direction of the global  $XY$  coordinate system;  $\theta$  is the dip angle of the inclined elliptic inclusion relative to the global coordinate system.

Similarly, if the pore-fluid flow in the unperturbed far field is vertical, its corresponding components in the local  $xy$  coordinate system can be expressed as follows.

$$U_x = U_Y \sin \theta, \quad U_y = U_Y \cos \theta \quad (2)$$

where  $U_x$  and  $U_y$  are the pore-fluid velocity components of the far field in the  $x$  and  $y$  directions of the local  $xy$  coordinate system;  $U_Y$  is the vertical pore-fluid velocity component of the far field in the  $Y$  direction of the global  $XY$  coordinate system;  $\theta$  is the dip angle of the inclined elliptic inclusion.

If the pore-fluid is incompressible, the governing equation of pore-fluid pressure in a pore-fluid-saturated porous medium can be described as a Laplace equation so that the superposition principle is valid in deriving analytical solutions for pore-fluid flow around an inclined elliptic inclusion. This indicates that if analytical solutions for pore-fluid flow around an inclined elliptic inclusion can be derived in the cases of the inflow pore-fluid velocity being parallel to the long and short axes of the inclined elliptic inclusion respectively, then analytical solutions for pore-fluid flow around an inclined elliptic inclusion can be obtained for any inflow pore-fluid velocity in the unperturbed far field by superposition. For this reason, an isolated elliptic inclusion (shown in Fig. 2) in the local  $xy$  and  $\xi\eta$  coordinate systems is considered in the derivation of the analytical solution for the pore-fluid flow around the elliptic inclusion. We assume that the system is comprised of pore-fluid saturated, isotropic porous rocks, although the

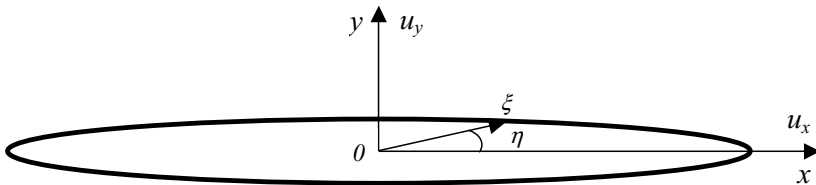


**Figure 2.** Description of an elliptic inclusion in two local coordinate systems.

permeability of the elliptic inclusion is different from that of the surrounding rocks. In the first case, we also assume that pore-fluid flow in the unperturbed far field away from the elliptic inclusion is uniform and in the  $y$  direction only ( $U_x = 0$ ) such that the short axis of the elliptic inclusion is parallel to the inflow direction in the undisturbed far field. The steady-state governing equations for such a problem can be expressed in the  $xy$  coordinate system as

$$\frac{\partial u_x}{\partial x} + \frac{\partial u_y}{\partial y} = 0 \tag{3}$$

$$u_x = -\frac{K}{\mu} \frac{\partial p}{\partial x}$$

$$u_y = -\frac{K}{\mu} \frac{\partial p}{\partial y} \tag{4}$$

where  $u_x$  and  $u_y$  are the velocity components in the  $x$  and  $y$  direction;  $p$  is the excess pore-fluid pressure (i.e. the total pore-fluid pressure minus the hydrostatic pore-fluid pressure);  $\mu$  is the dynamic viscosity of pore-fluid;  $K$  is the intrinsic permeability of the isotropic porous rocks. It needs to be pointed out that  $K = K_{in}$  for the elliptic inclusion and  $K = K_{out}$  for the surrounding rock of the elliptic inclusion, where  $K_{in}$  and  $K_{out}$  are the intrinsic permeability of the elliptic inclusion and its surrounding rock, respectively.

Substituting Eq. (4) into Eq. (3) yields the following equation:

$$\frac{\partial^2 p}{\partial x^2} + \frac{\partial^2 p}{\partial y^2} = 0 \tag{5}$$

Note that in order to facilitate the derivation of analytical solutions for the problem considered, Eq. (5) is rewritten in the  $\xi\eta$  coordinate system using the following coordinate mapping.

$$x = \cosh \xi \cos \eta, \quad y = \sinh \xi \sin \eta \quad (0 \leq \xi < \infty, 0 \leq \eta \leq 2\pi), \tag{6}$$

Using the coordinate mapping relationship expressed in Eq. (6), the following matrix equation can be obtained.

$$\begin{Bmatrix} \frac{\partial p}{\partial x} \\ \frac{\partial p}{\partial y} \end{Bmatrix} = \frac{\begin{bmatrix} \sinh \xi \cos \eta & -\cosh \xi \sin \eta \\ \cosh \xi \sin \eta & \sinh \xi \cos \eta \end{bmatrix}}{(\sinh^2 \xi \cos^2 \eta + \cosh^2 \xi \sin^2 \eta)} \begin{Bmatrix} \frac{\partial p}{\partial \xi} \\ \frac{\partial p}{\partial \eta} \end{Bmatrix} \tag{7}$$

Similarly, the following equation holds true for the stream function around the elliptic inclusion.

$$\left\{ \begin{array}{l} \frac{\partial \psi}{\partial x} \\ \frac{\partial \psi}{\partial y} \end{array} \right\} = \frac{\left[ \begin{array}{cc} \sinh \xi \cos \eta & -\cosh \xi \sin \eta \\ \cosh \xi \sin \eta & \sinh \xi \cos \eta \end{array} \right]}{(\sinh^2 \xi \cos^2 \eta + \cosh^2 \xi \sin^2 \eta)} \left\{ \begin{array}{l} \frac{\partial \psi}{\partial \xi} \\ \frac{\partial \psi}{\partial \eta} \end{array} \right\} \quad (8)$$

Where  $\psi$  is the stream function of the pore-fluid flow system.

Mathematically, we can prove that Eq. (6) is a conformal mapping so that Eq. (5) can be expressed as follows.

$$\left( \frac{\partial^2 p}{\partial \xi^2} + \frac{\partial^2 p}{\partial \eta^2} \right) = 0 \quad (9)$$

Equation (9) is the governing equation of the excess pore-fluid pressure in the local  $\xi\eta$  coordinate system.

### Inflow of the Far Field being Parallel to the $y$ Direction of the Local $xy$ Coordinate System

In this case, the boundary condition of the pore-fluid flow problem can be mathematically expressed in the following form.

$$p_{in} = p_{out} \quad (\text{at } \xi = \xi_0) \quad (10)$$

$$K_{in} \frac{\partial p_{in}}{\partial \xi} = K_{out} \frac{\partial p_{out}}{\partial \xi} \quad (\text{at } \xi = \xi_0) \quad (11)$$

$$\lim_{\xi \rightarrow \infty} p_{out} = -\omega_y \sinh \xi \sin \eta \quad (12)$$

where  $p_{in}$  and  $p_{out}$  are the excess pore-fluid pressure inside and outside the elliptic inclusion respectively;  $\xi_0$  is the boundary of the elliptic inclusion;  $K_{in}$  and  $K_{out}$  are the intrinsic permeability of the porous medium inside and outside the elliptic inclusion;  $\omega_y = \left| \frac{\partial p}{\partial y} \right|$  is the amplitude of the excess pore-fluid pressure gradient in the  $y$  direction of the far field.

Equation (10) expresses the excess pore-fluid pressure continuity at the boundary between the elliptic inclusion and the surrounding rock, while Eq. (11) expresses the pore-fluid flux continuity in the normal direction of this boundary. Equation (12) is used to express the distribution of the excess pore-fluid pressure in the far field, namely the boundary condition of the excess pore-fluid pressure at infinity.

The general solution to the excess pore-fluid pressure inside and outside the elliptic inclusion due to an inflow in the  $y$  direction of the far field can be expressed as

$$p_{in} = -\omega_y C_1 \sinh \xi \sin \eta \tag{13}$$

$$p_{out} = -\omega_y \sinh \xi \sin \eta + \omega_y C_2 e^{-(\xi-\xi_0)} \sin \eta \tag{14}$$

where  $C_1$  and  $C_2$  are two constants to be determined by the boundary conditions of the problem.

Substituting Eqs. (13) and (14) into Eqs. (10) and (11) yields the following equations.

$$(1 - C_1) \sinh \xi_0 - C_2 = 0 \tag{15}$$

$$\left( \frac{K_{in}}{K_{out}} C_1 - 1 \right) \cosh \xi_0 - C_2 = 0 \tag{16}$$

Solving Eqs. (15) and (16) simultaneously yields the following expressions for  $C_1$  and  $C_2$ .

$$C_1 = \frac{1 + \beta}{1 + \alpha\beta}, \quad C_2 = \frac{(\alpha - 1)a}{1 + \alpha\beta} \tag{17}$$

where

$$\beta = \frac{\cosh \xi_0}{\sinh \xi_0} = \frac{a}{b}, \quad \alpha = \frac{K_{in}}{K_{out}} \tag{18}$$

where  $\alpha$  is the permeability ratio of the elliptic inclusion to its surrounding rock;  $\beta$  is the aspect ratio of the elliptic inclusion;  $a = \cosh \xi_0$  and  $b = \sinh \xi_0$  are half the length of the long and short axes of the elliptic inclusion.

Note that the following mathematical equalities exist for the elliptic inclusion.

$$e^{\xi_0} = \cosh \xi_0 + \sinh \xi_0 = a + b, \quad e^{\xi_0} = \frac{1}{e^{-\xi_0}} = \frac{1}{\cosh \xi_0 - \sinh \xi_0} = \frac{1}{a - b} \tag{18a}$$

Using these two equalities can yield the following equations.

$$a^2 - b^2 = 1, \quad a = \frac{\beta}{\sqrt{\beta^2 - 1}}, \quad b = \frac{1}{\sqrt{\beta^2 - 1}} \tag{18b}$$

Considering Eqs. (4), (7), (13), (14), (17) and (18) yields the corresponding analytical solution to the pore-fluid velocity as follows.

$$u_x^{in} = 0 \quad (\xi \leq \xi_0) \tag{19}$$

$$u_y^{in} = \frac{\omega_y K_{in}}{\mu} \left( \frac{1 + \beta}{1 + \alpha\beta} \right) \quad (\xi \leq \xi_0) \tag{20}$$

$$u_x^{out} = \frac{\omega_y K_{out}}{\mu} \left[ \left( \frac{\alpha - 1}{1 + \alpha\beta} \right) \frac{(\sinh \xi + \cosh \xi) \sin \eta \cos \eta e^{-(\xi - \xi_0)}}{\sinh^2 \xi \cos^2 \eta + \cosh^2 \xi \sin^2 \eta} \right] \quad (\xi \geq \xi_0) \tag{21}$$

$$u_y^{out} = \frac{\omega_y K_{out}}{\mu} \left[ 1 + \left( \frac{\alpha - 1}{1 + \alpha\beta} \right) \frac{(\cosh \xi \sin^2 \eta - \sinh \xi \cos^2 \eta) e^{-(\xi - \xi_0)}}{\sinh^2 \xi \cos^2 \eta + \cosh^2 \xi \sin^2 \eta} \right] \quad (\xi \geq \xi_0) \tag{22}$$

where the superscripts, in and out, represent the inside and outside domains of the elliptic inclusion respectively.

Equation (20) indicates that as the inclusion becomes perfectly impermeable, the intrinsic permeability of the inclusion goes to zero so that the pore-fluid velocity within the elliptic inclusion approaches zero. Since the intrinsic permeability must have a value between zero (in the case of perfectly impermeable) and one (in the case of perfectly permeable),  $\alpha \rightarrow 0$  as  $K_{in} \rightarrow 0$ . This implies that if  $\alpha \rightarrow \infty$ , then the surrounding rock must be perfectly impermeable so that  $K_{out} \rightarrow 0$ . In this case, Eq. (20) can be rewritten as  $u_y^{in} = \frac{\omega_y \alpha K_{out}}{\mu} \left( \frac{1 + \beta}{1 + \alpha\beta} \right)$ , which tends to a value of  $\frac{\omega_y K_{out}}{\mu \beta}$  as  $\alpha \rightarrow \infty$ . Clearly,  $u_y^{in} \rightarrow 0$  as  $K_{out} \rightarrow 0$ . This indicates that if the surrounding rock is perfectly impermeable, the pore-fluid velocity within the elliptic inclusion expressed by Eq. (20) approaches the far field velocity, which has a limiting value of zero. If the surrounding rock is not perfectly impermeable (i.e. the inclusion is not perfectly permeable), the pore-fluid velocity within the elliptic inclusion is, strictly speaking, not equal to the far field velocity unless the aspect ratio of the elliptic inclusion approaches infinite (i.e.  $\beta \rightarrow \infty$ ). This is consistent with the previous solutions for perfectly permeable and very thin but very long inclusions (Phillips, 1991).

In order to quantitatively describe the flow-focusing effect, a flow-focusing factor due to this elliptic inclusion is defined as

$$\lambda_y = \frac{u_y^{in}}{\lim_{\xi \rightarrow \infty} u_y^{out}} = \frac{\alpha(1 + \beta)}{1 + \alpha\beta} \tag{23}$$

where  $\lambda_y$  is the pore-fluid-flow focusing factor of the elliptic inclusion in the case of the inflow being in the y direction in the far field of the local xy coordinate system.

The pore-fluid-flow focusing factor of an elliptic inclusion is dependent on the aspect ratio representing the specific geometry of the elliptic inclusion and the permeability ratio representing the hydrodynamic property of the elliptic inclusion. If the aspect ratio of an elliptic inclusion is equal to unity, then the elliptic inclusion becomes a circular one so that the pore-fluid-flow focusing factor of the elliptic inclusion degenerates into that of a circular inclusion, as obtained in a previous study (Zhao and others, 1999).

From potential flow theory (Gerhart, Gross, and Hochstein, 1993), the following relationship between the stream function  $\psi$  and the pore-fluid velocity exists:

$$\begin{aligned} \frac{\partial \psi}{\partial y} &= u_x \\ \frac{\partial \psi}{\partial x} &= -u_y \end{aligned} \tag{24}$$

Considering Eqs. (4), (7), (8) and (24) yields the analytical solution for the stream function due to the elliptic inclusion as follows:

$$\begin{aligned} \psi_{in} &= -\frac{\omega_y K_{in}}{\mu} \left( \frac{1 + \beta}{1 + \alpha\beta} \right) \cosh \xi \cos \eta + C \quad (\xi \leq \xi_0) \\ \psi_{out} &= -\frac{\omega_y K_{out}}{\mu} \left[ \cosh \xi \cos \eta + \left( \frac{(\alpha - 1)a}{1 + \alpha\beta} \right) e^{-(\xi - \xi_0)} \cos \eta \right] + C \quad (\xi \geq \xi_0) \end{aligned} \tag{25}$$

where  $\psi_{in}$  and  $\psi_{out}$  are the stream functions inside and outside the elliptic inclusion respectively;  $C$  is an arbitrary constant.

For a perfectly permeable inclusion relative to the surrounding rock, the permeability ratio of the inclusion approaches infinite (i.e.  $\alpha \rightarrow \infty$ ). If this perfectly permeable inclusion is very thin but very long, then the aspect ratio of the inclusion approaches infinite (i.e.  $\beta \rightarrow \infty$ ). In this particular case, Eq. (25) can be rewritten as follows.

$$\begin{aligned} \lim_{\alpha \rightarrow \infty, \beta \rightarrow \infty} \psi_{out} &= -\frac{\omega_y K_{out}}{\mu} \lim_{\alpha \rightarrow \infty, \beta \rightarrow \infty} \left[ \cosh \xi \cos \eta + \left( \frac{(\alpha - 1)a}{1 + \alpha\beta} \right) e^{-(\xi - \xi_0)} \cos \eta \right] \\ &= -\frac{\omega_y K_{out}}{\mu} \cos \eta \lim_{\beta \rightarrow \infty} \left[ \cosh \xi + \left( \frac{1}{\beta + 1} \right) e^{-\xi} \right] \\ &= -\frac{\omega_y K_{out}}{\mu} \cosh \xi \cos \eta = U_{y,x} \end{aligned} \tag{25a}$$

Note that Eq. (25a) is exactly the same as the previous solution derived for the limiting case of a perfectly permeable and very thin but very long inclusion (Phillips, 1991).

**Inflow of the Far Field being Parallel to the  $x$  Direction  
of the Local  $xy$  Coordinate System**

In this case, the boundary condition of the pore-fluid flow problem can be mathematically expressed in the following form.

$$p_{in} = p_{out} \quad (\text{at } \xi = \xi_0) \tag{26}$$

$$K_{in} \frac{\partial p_{in}}{\partial \xi} = K_{out} \frac{\partial p_{out}}{\partial \xi} \quad (\text{at } \xi = \xi_0) \tag{27}$$

$$\lim_{\xi \rightarrow \infty} p_{out} = -\omega_x \cosh \xi \cos \eta \tag{28}$$

where  $p_{in}$  and  $p_{out}$  are the excess pore-fluid pressure inside and outside the elliptic inclusion respectively;  $\xi_0$  is the boundary of the elliptic inclusion;  $K_{in}$  and  $K_{out}$  are the intrinsic permeability of the porous medium inside and outside the elliptic inclusion;  $\omega_x = |\frac{\partial p}{\partial x}|$  is the amplitude of the excess pore-fluid pressure gradient in the  $x$  direction of the far field.

Following the same procedures as used above, the analytical solutions for the stream function, excess pore-fluid pressure and velocity around the buried elliptic inclusion can be expressed as follows.

$$\psi_{in} = \frac{\omega_x K_{in}}{\mu} \left( \frac{\beta + 1}{\beta + \alpha} \right) \sinh \xi \sin \eta + C \quad (\xi \leq \xi_0) \tag{29}$$

$$\psi_{out} = \frac{\omega_x K_{out}}{\mu} \left[ \sinh \xi + \frac{(\alpha - 1)a}{\beta + \alpha} e^{-(\xi - \xi_0)} \right] \sin \eta + C \quad (\xi \geq \xi_0) \tag{30}$$

$$p_{in} = -\omega_x \left( \frac{\beta + 1}{\beta + \alpha} \right) \cosh \xi \cos \eta \quad (\xi \leq \xi_0) \tag{31}$$

$$p_{out} = -\omega_x \cosh \xi \cos \eta + \omega_x \frac{(\alpha - 1)a}{\beta + \alpha} e^{-(\xi - \xi_0)} \cos \eta \quad (\xi \geq \xi_0) \tag{32}$$

$$u_x^{in} = \frac{\omega_x K_{in}}{\mu} \left( \frac{\beta + 1}{\beta + \alpha} \right) \quad (\xi \leq \xi_0) \tag{33}$$

$$u_y^{in} = 0 \quad (\xi \leq \xi_0) \tag{34}$$

$$u_x^{out} = \frac{\omega_x K_{out}}{\mu} \left[ 1 + \left( \frac{(\alpha - 1)a}{\beta + \alpha} \right) \frac{(\sinh \xi \cos^2 \eta - \cosh \xi \sin^2 \eta)e^{-(\xi - \xi_0)}}{\sinh^2 \xi \cos^2 \eta + \cosh^2 \xi \sin^2 \eta} \right] \quad (\xi \geq \xi_0) \tag{35}$$

$$u_y^{out} = \frac{\omega_x K_{out}}{\mu} \left[ \left( \frac{(\alpha - 1)a}{\beta + \alpha} \right) \frac{(\cosh \xi \sin \eta \cos \eta + \sinh \xi \sin \eta \cos \eta)e^{-(\xi - \xi_0)}}{\sinh^2 \xi \cos^2 \eta + \cosh^2 \xi \sin^2 \eta} \right] \quad (\xi \geq \xi_0) \tag{36}$$

where  $\beta$  is the aspect ratio of the elliptic inclusion;  $\alpha$  is the permeability ratio of the elliptic inclusion to its surrounding rock.

Note that Since the intrinsic permeability must have a value between zero (in the case of perfectly impermeable) and one (in the case of perfectly permeable),  $\alpha \rightarrow 0$  results in  $K_{in} \rightarrow 0$ . In such a case, Eq. (33) indicates that as the inclusion becomes perfectly impermeable, the pore-fluid velocity within the elliptic inclusion approaches zero.

In order to compare the present analytical solution with the previous one (Phillips, 1991), it is necessary to examine the behaviour of Eq. (30) in the limiting case. If an elliptic inclusion is perfectly permeable relative to the surrounding rock, the permeability ratio of the inclusion approaches infinite (i.e.  $\alpha \rightarrow \infty$ ). If this perfectly permeable inclusion is also very thin but very long, then the aspect ratio of the inclusion approaches infinite (i.e.  $\beta \rightarrow \infty$ ). In this particular case, Eq. (30) can be rewritten as follows.

$$\begin{aligned} \lim_{\alpha \rightarrow \infty, \beta \rightarrow \infty} \psi_{out} &= \frac{\omega_x K_{out}}{\mu} \lim_{\alpha \rightarrow \infty, \beta \rightarrow \infty} \left[ \sinh \xi + \left( \frac{(\alpha - 1)a}{\alpha + \beta} \right) e^{-(\xi - \xi_0)} \right] \sin \eta \\ &= \frac{\omega_x K_{out}}{\mu} \sin \eta \lim_{\beta \rightarrow \infty} \left[ \sinh \xi + \left( \frac{\beta}{\beta + 1} \right) e^{-\xi} \right] \\ &= \frac{\omega_x K_{out}}{\mu} \cosh \xi \sin \eta = U_x \cosh \xi \sin \eta \end{aligned} \tag{36a}$$

Since Phillips (1991) used the conformal mapping of the form of  $x = d \cosh \xi \cos \eta$  and  $y = d \sinh \xi \sin \eta$  (note that  $d$ , instead of  $a$ , is used here to avoid unnecessary confusion) in deriving the previous solutions, the value of  $d$  needs to be set to one so that the present solution can be compared with the previous solution (Phillips, 1991) in the limiting case. Clearly, Eq. (36a) is identical to the previous solution derived for the limiting case of a perfectly permeable and very thin but very long inclusion (Phillips, 1991).

In this case, the analytical solution to the pore-fluid-flow focusing factor of the elliptic inclusion can be expressed as

$$\lambda_x = \frac{u_x^{in}}{\lim_{\xi \rightarrow \infty} u_x^{out}} = \frac{\alpha(\beta + 1)}{\beta + \alpha} \tag{37}$$

where  $\lambda_x$  is the pore-fluid-flow focusing factor of the elliptic inclusion in the case of the inflow being parallel to the  $x$  direction in the far field of the local  $xy$  coordinate system.

**Inflow of the Far Field being Parallel to the  $X$  Direction  
of the Global  $XY$  Coordinate System**

Since the governing equation of excess pore-fluid pressure in a pore-fluid-saturated porous medium is described using Eq. (9), which is a linear second-order partial differential equation, the superposition principle is valid in deriving analytical solutions for pore-fluid flow around an inclined elliptic inclusion when the inflow of the far field is parallel to the  $X$  direction of the global  $XY$  coordinate system.

Substituting the Darcy’s law into Eq. (1) yields the following equations.

$$-\frac{K_{out}}{\mu}\omega_x = -\frac{K_{out}}{\mu}\omega_X \cos \theta, \quad -\frac{K_{out}}{\mu}\omega_y = \frac{K_{out}}{\mu}\omega_X \sin \theta \tag{38}$$

where  $\omega_x$  and  $\omega_y$  are the amplitudes of the excess pore-fluid pressure gradient in the  $x$  and  $y$  directions of the local  $xy$  coordinate system in the far field;  $\omega_X$  is the amplitude of the excess pore-fluid pressure gradient in the  $X$  direction of the global  $XY$  coordinate system in the far field.

Equation (38) can be straightforwardly written as follows.

$$\omega_x = \omega_X \cos \theta, \quad \omega_y = -\omega_X \sin \theta \tag{39}$$

Superposing the analytical solutions derived in the previous two sub-sections yields the analytical solutions for pore-fluid flow around an inclined elliptic inclusion when the inflow of the far field is parallel to the  $X$  direction of the global  $XY$  coordinate system.

$$\psi_{in} = \frac{\omega_X K_{in}}{\mu} \left[ \left( \frac{\beta + 1}{\beta + \alpha} \right) \sinh \xi \sin \eta \cos \theta + \left( \frac{1 + \beta}{1 + \alpha\beta} \right) \cosh \xi \cos \eta \sin \theta \right] + C \tag{40}$$

$(\xi \leq \xi_0)$

$$\psi_{out} = \frac{\omega_X K_{out}}{\mu} \left\{ \left[ \sinh \xi + \frac{(\alpha - 1)a}{\beta + \alpha} e^{-(\xi - \xi_0)} \right] \sin \eta \cos \theta + \left[ \cosh \xi + \left( \frac{\alpha - 1}{1 + \alpha\beta} \right) e^{-(\xi - \xi_0)} \right] \cos \eta \sin \theta \right\} + C \tag{41}$$

$(\xi \geq \xi_0)$

$$p_{in} = -\omega_X \left( \frac{\beta + 1}{\beta + \alpha} \right) \cosh \xi \cos \eta \cos \theta + \omega_X \left( \frac{1 + \beta}{1 + \alpha\beta} \right) \sinh \xi \sin \eta \sin \theta \quad (\xi \leq \xi_0) \tag{42}$$

$$p_{out} = -\omega_X \left[ \cosh \xi - \frac{(\alpha - 1)a}{\beta + \alpha} e^{-(\xi - \xi_0)} \right] \cos \eta \cos \theta + \omega_X \left[ \sinh \xi - \omega_X \left( \frac{(\alpha - 1)a}{1 + \alpha\beta} \right) e^{-(\xi - \xi_0)} \right] \sin \eta \sin \theta \quad (\xi \geq \xi_0) \tag{43}$$

$$u_x^{in} = \frac{\omega_X K_{in}}{\mu} \left( \frac{\beta + 1}{\beta + \alpha} \right) \cos \theta \quad (\xi \leq \xi_0) \tag{44}$$

$$u_y^{in} = -\frac{\omega_X K_{in}}{\mu} \left( \frac{1 + \beta}{1 + \alpha\beta} \right) \sin \theta \quad (\xi \leq \xi_0) \tag{45}$$

$$u_x^{out} = \frac{\omega_X K_{out}}{\mu} \left[ 1 + \left( \frac{(\alpha - 1)a}{\beta + \alpha} \right) \frac{(\sinh \xi \cos^2 \eta - \cosh \xi \sin^2 \eta) e^{-(\xi - \xi_0)}}{\sinh^2 \xi \cos^2 \eta + \cosh^2 \xi \sin^2 \eta} \right] \cos \theta - \frac{\omega_X K_{out}}{\mu} \left[ \left( \frac{(\alpha - 1)a}{1 + \alpha\beta} \right) \frac{(\sinh \xi + \cosh \xi) \sin \eta \cos \eta e^{-(\xi - \xi_0)}}{\sinh^2 \xi \cos^2 \eta + \cosh^2 \xi \sin^2 \eta} \right] \sin \theta \quad (\xi \geq \xi_0) \tag{46}$$

$$u_y^{out} = \frac{\omega_X K_{out}}{\mu} \left[ \left( \frac{(\alpha - 1)a}{\beta + \alpha} \right) \frac{(\cosh \xi \sin \eta \cos \eta + \sinh \xi \sin \eta \cos \eta) e^{-(\xi - \xi_0)}}{\sinh^2 \xi \cos^2 \eta + \cosh^2 \xi \sin^2 \eta} \right] \cos \theta - \frac{\omega_X K_{out}}{\mu} \left[ 1 + \left( \frac{(\alpha - 1)a}{1 + \alpha\beta} \right) \frac{(\cosh \xi \sin^2 \eta - \sinh \xi \cos^2 \eta) e^{-(\xi - \xi_0)}}{\sinh^2 \xi \cos^2 \eta + \cosh^2 \xi \sin^2 \eta} \right] \sin \theta \quad (\xi \geq \xi_0) \tag{47}$$

In order to derive the pore-fluid-flow focusing factor of the inclined elliptic inclusion in the case of the inflow being parallel to the  $X$  direction in the far field of the global  $XY$  coordinate system, the following equality needs to be considered.

$$\lambda_X = \frac{u_x^{in} \cos \theta - u_y^{in} \sin \theta}{U_X} = \frac{u_x^{in} \cos^2 \theta}{U_X \cos \theta} - \frac{u_y^{in} \sin^2 \theta}{U_X \sin \theta} = \lim_{\xi \rightarrow \infty} \frac{u_x^{in} \cos^2 \theta}{u_x^{out}} + \lim_{\xi \rightarrow \infty} \frac{u_y^{in} \sin^2 \theta}{u_y^{out}} \tag{48}$$

Inserting Eqs. (23) and (37) into Eq. (48) yields the following equation.

$$\lambda_X = \lambda_x \cos^2 \theta + \lambda_y \sin^2 \theta \tag{49}$$

where  $\lambda_x$  and  $\lambda_y$  are the pore-fluid-flow focusing factors of the inclined elliptic inclusion in the case of the inflow being parallel to the  $x$  and  $y$  directions in the far field of the local  $xy$  coordinate system;  $\lambda_X$  is the pore-fluid-flow focusing factor of the inclined elliptic inclusion in the case of the inflow being parallel to the  $X$  direction in the far field of the global  $XY$  coordinate system.

Clearly, Eq. (49) indicates that if the inflow of the far field is not parallel to either the long axis or the short axis of an inclined elliptic inclusion, the pore-fluid-flow focusing factor is also dependent on the dip angle of the inclined elliptic inclusion.

**Inflow of the Far Field being Parallel to the Y Direction  
of the Global XY Coordinate System**

Similarly, the superposition principle is valid in deriving analytical solutions for pore-fluid flow around an inclined elliptic inclusion when the inflow of the far field is parallel to the  $Y$  direction of the global  $XY$  coordinate system.

Substituting the Darcy’s law into Eq. (2) yields the following equations.

$$-\frac{K_{out}}{\mu}\omega_x = -\frac{K_{out}}{\mu}\omega_Y \sin \theta, \quad -\frac{K_{out}}{\mu}\omega_y = -\frac{K_{out}}{\mu}\omega_Y \cos \theta \quad (50)$$

where  $\omega_x$  and  $\omega_y$  are the amplitudes of the excess pore-fluid pressure gradient in the  $x$  and  $y$  directions of the local  $xy$  coordinate system in the far field;  $\omega_Y$  is the amplitude of the excess pore-fluid pressure gradient in the  $Y$  direction of the global  $XY$  coordinate system in the far field.

Equation (50) can be straightforwardly written as follows.

$$\omega_x = \omega_Y \sin \theta, \quad \omega_y = \omega_Y \cos \theta \quad (51)$$

Superposing the analytical solutions derived in the previous two sub-sections yields the analytical solutions for pore-fluid flow around an inclined elliptic inclusion when the inflow of the far field is parallel to the  $Y$  direction of the global  $XY$  coordinate system.

$$\psi_{in} = \frac{\omega_Y K_{in}}{\mu} \left[ \left( \frac{\beta + 1}{\beta + \alpha} \right) \sinh \xi \sin \eta \sin \theta - \left( \frac{1 + \beta}{1 + \alpha\beta} \right) \cosh \xi \cos \eta \cos \theta \right] + C \quad (\xi \leq \xi_0) \quad (52)$$

$$\psi_{out} = \frac{\omega_Y K_{out}}{\mu} \left\{ \left[ \sinh \xi + \frac{(\alpha - 1)a}{\beta + \alpha} e^{-(\xi - \xi_0)} \right] \sin \eta \sin \theta - \left[ \cosh \xi + \left( \frac{\alpha - 1}{1 + \alpha\beta} \right) a e^{-(\xi - \xi_0)} \right] \cos \eta \cos \theta \right\} + C \quad (\xi \geq \xi_0) \quad (53)$$

$$p_{\text{in}} = -\omega_Y \left( \frac{\beta + 1}{\beta + \alpha} \right) \cosh \xi \cos \eta \sin \theta - \omega_Y \left( \frac{1 + \beta}{1 + \alpha\beta} \right) \sinh \xi \sin \eta \cos \theta \quad (\xi \leq \xi_0) \quad (54)$$

$$p_{\text{out}} = -\omega_Y \left[ \cosh \xi - \frac{(\alpha - 1)a}{\beta + \alpha} e^{-(\xi - \xi_0)} \right] \cos \eta \sin \theta - \omega_Y \times \left[ \sinh \xi - \omega_X \left( \frac{(\alpha - 1)a}{1 + \alpha\beta} \right) e^{-(\xi - \xi_0)} \right] \sin \eta \cos \theta \quad (\xi \geq \xi_0) \quad (55)$$

$$u_x^{\text{in}} = \frac{\omega_Y K_{\text{in}}}{\mu} \left( \frac{\beta + 1}{\beta + \alpha} \right) \sin \theta \quad (\xi \leq \xi_0) \quad (56)$$

$$u_y^{\text{in}} = \frac{\omega_Y K_{\text{in}}}{\mu} \left( \frac{1 + \beta}{1 + \alpha\beta} \right) \cos \theta \quad (\xi \leq \xi_0) \quad (57)$$

$$u_x^{\text{out}} = \frac{\omega_Y K_{\text{out}}}{\mu} \left[ 1 + \left( \frac{(\alpha - 1)a}{\beta + \alpha} \right) \frac{(\sinh \xi \cos^2 \eta - \cosh \xi \sin^2 \eta) e^{-(\xi - \xi_0)}}{\sinh^2 \xi \cos^2 \eta + \cosh^2 \xi \sin^2 \eta} \right] \sin \theta + \frac{\omega_Y K_{\text{out}}}{\mu} \left[ \left( \frac{(\alpha - 1)a}{1 + \alpha\beta} \right) \frac{(\sinh \xi + \cosh \xi) \sin \eta \cos \eta e^{-(\xi - \xi_0)}}{\sinh^2 \xi \cos^2 \eta + \cosh^2 \xi \sin^2 \eta} \right] \cos \theta \quad (\xi \geq \xi_0) \quad (58)$$

$$u_y^{\text{out}} = \frac{\omega_Y K_{\text{out}}}{\mu} \left[ \left( \frac{(\alpha - 1)a}{\beta + \alpha} \right) \frac{(\cosh \xi \sin \eta \cos \eta + \sinh \xi \sin \eta \cos \eta) e^{-(\xi - \xi_0)}}{\sinh^2 \xi \cos^2 \eta + \cosh^2 \xi \sin^2 \eta} \right] \sin \theta + \frac{\omega_Y K_{\text{out}}}{\mu} \left[ 1 + \left( \frac{(\alpha - 1)a}{1 + \alpha\beta} \right) \frac{(\cosh \xi \sin^2 \eta - \sinh \xi \cos^2 \eta) e^{-(\xi - \xi_0)}}{\sinh^2 \xi \cos^2 \eta + \cosh^2 \xi \sin^2 \eta} \right] \cos \theta \quad (\xi \geq \xi_0) \quad (59)$$

In order to derive the pore-fluid-flow focusing factor of the inclined elliptic inclusion in the case of the inflow being parallel to the  $Y$  direction in the far field of the global  $XY$  coordinate system, the following equality needs to be considered.

$$\lambda_Y = \frac{u_x^{\text{in}} \sin \theta + u_y^{\text{in}} \cos \theta}{U_Y} = \frac{u_x^{\text{in}} \sin^2 \theta}{U_Y \sin \theta} + \frac{u_y^{\text{in}} \cos^2 \theta}{U_Y \cos \theta} = \lim_{\xi \rightarrow \infty} \frac{u_x^{\text{in}} \sin^2 \theta}{u_x^{\text{out}}} + \lim_{\xi \rightarrow \infty} \frac{u_y^{\text{in}} \cos^2 \theta}{u_y^{\text{out}}} \quad (60)$$

Inserting Eqs. (23) and (37) into Eq. (60) yields the following equation.

$$\lambda_Y = \lambda_x \sin^2 \theta + \lambda_y \cos^2 \theta \quad (61)$$

where  $\lambda_x$  and  $\lambda_y$  are the pore-fluid-flow focusing factors of the inclined elliptic inclusion in the case of the inflow being parallel to the  $x$  and  $y$  directions in the far field of the local  $xy$  coordinate system;  $\lambda_Y$  is the pore-fluid-flow focusing factor of the inclined elliptic inclusion in the case of the inflow being parallel to the  $Y$  direction in the far field of the global  $XY$  coordinate system.

### APPLICATION EXAMPLES OF THE PRESENT ANALYTICAL SOLUTIONS

The present analytical solutions provide a useful tool for fundamentally understanding the general behaviour of pore-fluid flow around a buried inclined fault or crack within the crust of the Earth. For instance, the simple and elegant analytical solution for the flow focusing factor within a buried inclined fault can be used to understand how the pore-fluid flow is focused into the buried inclined fault with any dip angles. Since the pore-fluid-flow focusing factor is dependent on the angle between the long axis of the inclusion and the inflow direction in the unperturbed far field, we can consider all possible flow focusing situations by setting the inflow parallel to the  $X$  direction in the far field of the global  $XY$  coordinate system and varying the dip angle of the inclusion.

In the case of the dip angle being zero, Figure 3 shows the variation of analytical flow focusing factors with the aspect ratio of the inclusion for several different permeability ratios (i.e. PR in this figure) of the inclusion to its surrounding rock, while Figure 4 shows the variation of analytical flow focusing factors with the permeability ratio of the inclusion to its surrounding rock for several different

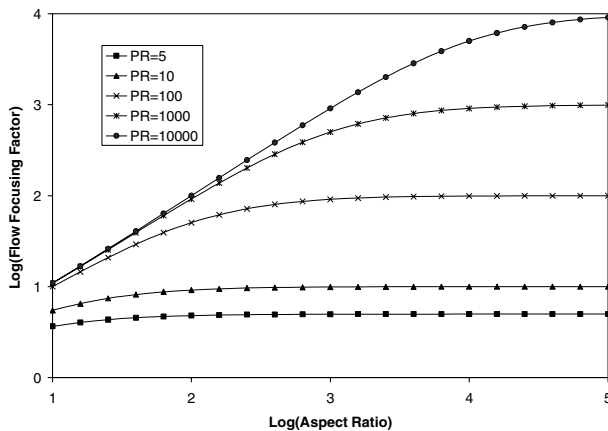


**Figure 3.** Variation of flow focusing factor with aspect ratio due to different permeability ratios (Inflow parallel to the long axis of the inclusion).

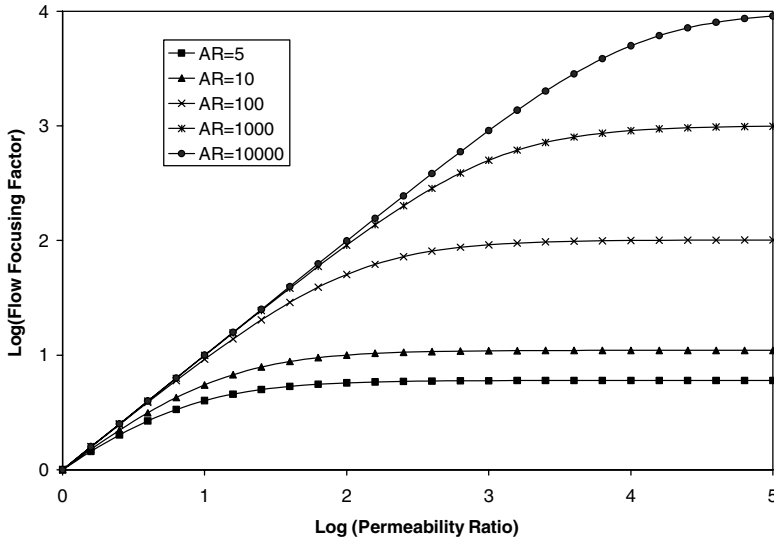


**Figure 4.** Variation of flow focusing factor with permeability ratio due to different aspect ratios (inflow parallel to the long axis of the inclusion).

aspect ratios (i.e. AR in this figure). It is obvious that for a given aspect ratio of the inclusion in the case of the dip angle being zero, the flow focusing factor increases with an increase in the permeability ratio of the inclusion to its surrounding rock until it reaches the corresponding limiting value. Similarly, for a given permeability ratio of the fault to its surrounding rock, the flow focusing factor increases with an increase in the aspect ratio of the inclusion until it reaches its corresponding limiting value. At this point, it is interesting to compare the present results with the previous ones in the limiting case (Phillips, 1991). For a perfectly permeable inclusion, the previous result indicated that the flow focusing factor ( $\lambda$ ) is equal to the aspect ratio ( $\beta$ ), namely  $\lambda = \beta$ . In the case of the aspect ratio (AR) being 10, 100, 1000 and 10000, the asymptotes of the corresponding logarithmic values of the flow focusing factor are 1, 2, 3 and 4 respectively. Since the present results of the flow focusing factor approaches the previous ones, it has been demonstrated that when the inflow is parallel to the long axis of the inclusion, the present results are consistent with the previous ones for perfectly permeable inclusions.

Figure 5 shows the streamline patterns around and within an elliptic inclusion of the aspect ratio being 5 due to three different permeabilities. In this figure, the dot points are used to show the outline of the elliptic inclusion. It can be observed that if the inclusion is permeable (i.e.  $\alpha = 10$ ), the pore-fluid flow is highly focused into the inclusion, while if the inclusion is perfectly impermeable ( $\alpha = 0$ ), the pore-fluid flow does not enter the inclusion. If the permeability of the inclusion is

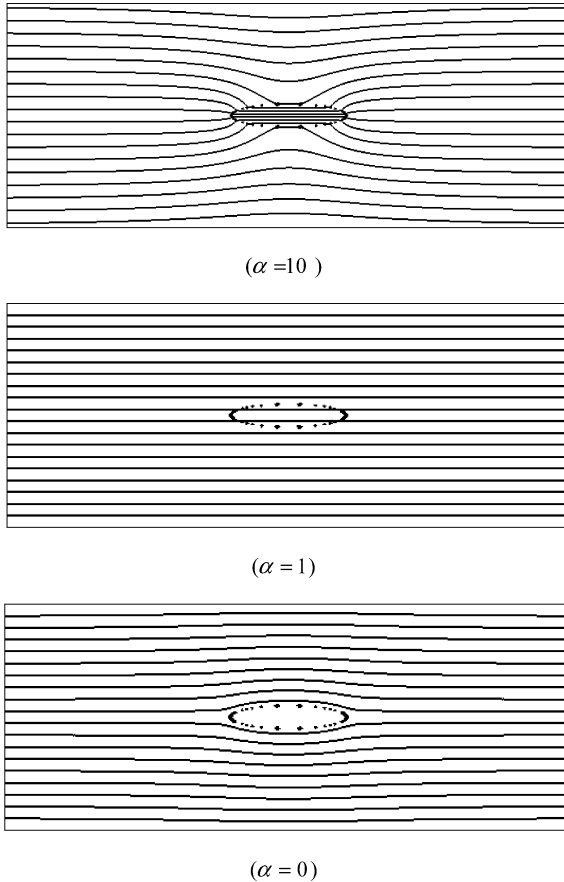


**Figure 5.** Streamline patterns around and within an elliptic inclusion due to different permeability ratios (Inflow parallel to the long axis of the inclusion).

the same as that of the surrounding rock ( $\alpha = 1$ ), the inclusion does not disturb the flow field. This indicates that the present solution agrees well with the previous ones for the streamline pattern around an elliptic inclusion (Phillips, 1991).

If the dip angle of the inclusion is  $90^\circ$ , the horizontal inflow in the unperturbed far field is parallel to the short axis of the inclusion. Figure 6 shows the variation of analytical flow focusing factors with the aspect ratio of the inclusion for several different permeability ratios (i.e. PR in this figure) of the inclusion to its surrounding rock, while Figure 7 shows the variation of analytical flow focusing factors with the permeability ratio of the inclusion to its surrounding rock for several different aspect ratios (i.e. AR in this figure) of the inclusion. Since the

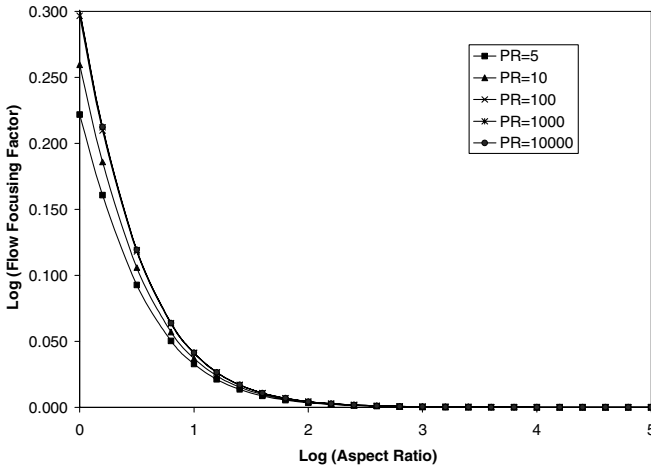


Figure 6. Variation of flow focusing factor with aspect ratio due to different permeability ratios (Inflow parallel to the short axis of the inclusion).

logarithm of the flow focusing factor is shown in the direction of the vertical axis (in Figs. 6 and 7), a logarithmic value of zero is in correspondence with the flow focusing factor of one. It is obvious that for a given permeability ratio, the pore-fluid-flow focusing factor approaches unity with the increase of the aspect ratio of the inclusion. The reason for this phenomenon is due to the fact that when the

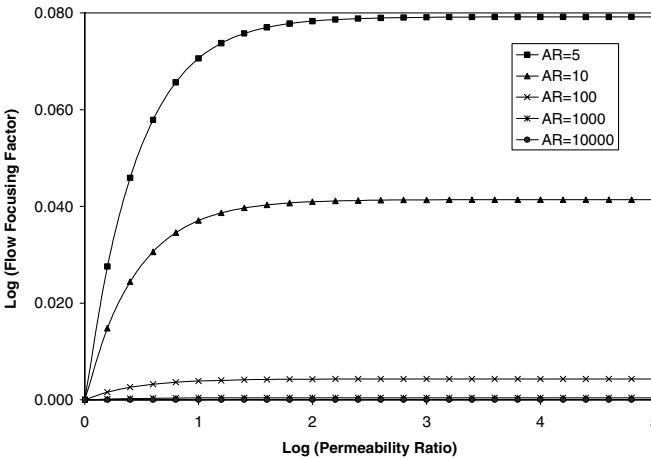
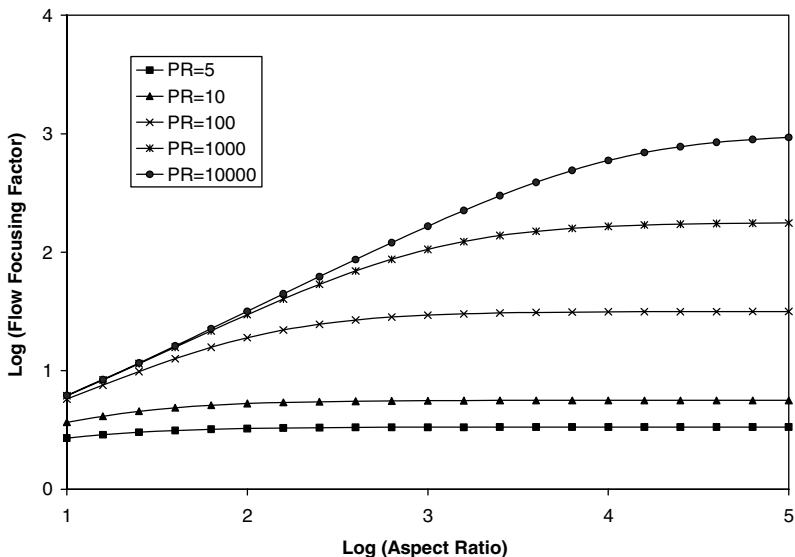


Figure 7. Variation of flow focusing factor with permeability ratio due to different aspect ratios (Inflow parallel to the short axis of the inclusion).



**Figure 8.** Variation of flow focusing factor with aspect ratio due to different permeability ratios (Inflow parallel to the  $X$  axis,  $\theta = 30^\circ$ ).

aspect ratio of an elliptic inclusion is infinite or very large, the inclusion behaves as an interface between surrounding rocks, so that the pore-fluid-flow focusing factor must be unity, as required by the pore-fluid mass conservation in the pore-fluid flow direction. For a given aspect ratio of the inclusion, the pore-fluid-flow focusing factor can also approach a limit value. Although this limit value may vary with different aspect ratios of the inclusion, it goes to unity as the aspect ratio approaches infinite. Thus, for a perfectly permeable and very thin but very long inclusion, the flow focusing factor is approaching one, implying that when the inflow is parallel to the short axis of the inclusion, the perfectly permeable inclusion does not perturb the flow field. This conclusion is consistent with that obtained from the previous study in the limiting case (Phillips, 1991). Comparing the analytical results in Figures 3 and 4 with those in Figures 6 and 7, clearly, the pore-fluid-flow focusing factors in the case of the inflow parallel to the short axis of the inclusion are much smaller than those in the case of the inflow parallel to the long axis of the inclusion. This indicates that the relative direction of the inflow in the far field to the long axis of an elliptic inclusion has a significant influence on the pore-fluid flow focusing factor of the inclusion.

In order to further examine the effect of the relative direction of the inflow in the far field to the long axis of an elliptic inclusion on the pore-fluid-flow focusing factor, three different intermediate dip angles, namely  $30^\circ$ ,  $45^\circ$  and  $60^\circ$ , are considered to produce the related analytical solutions. Figures 8, 10 and 12

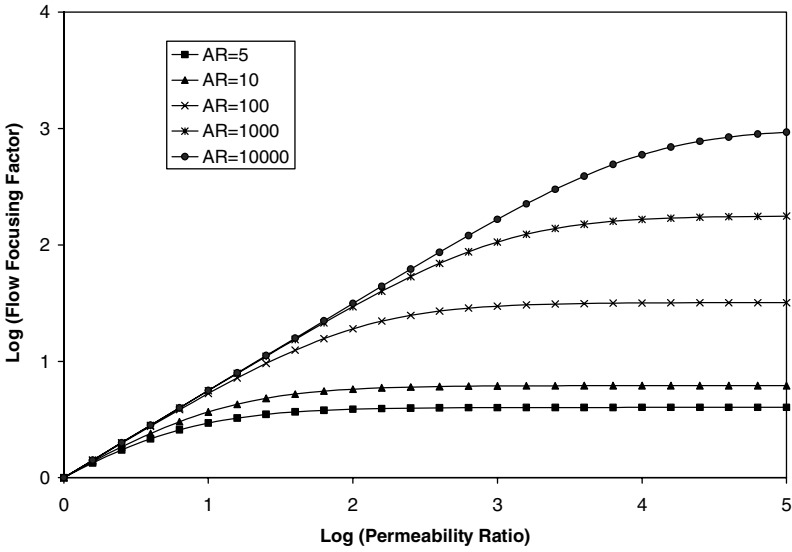


Figure 9. Variation of flow focusing factor with permeability ratio due to different aspect ratios (Inflow parallel to the X axis,  $\theta = 30^\circ$ ).

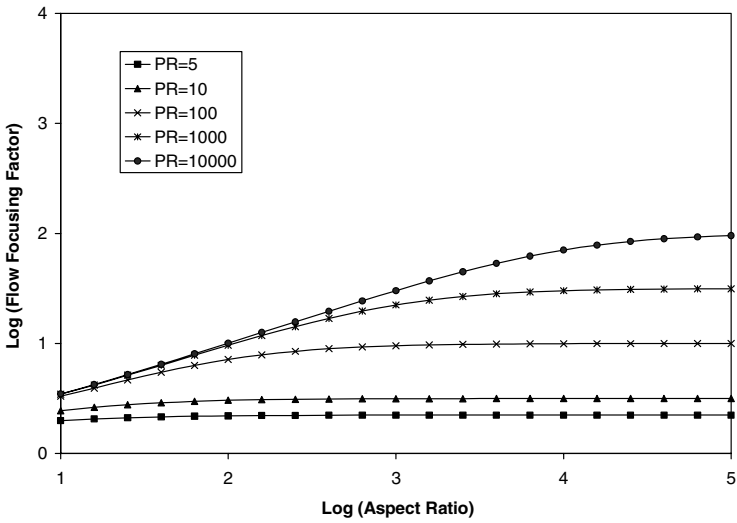
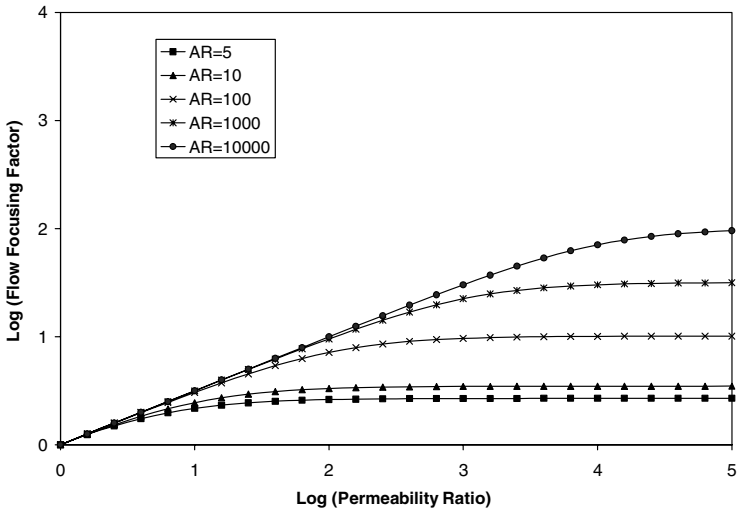
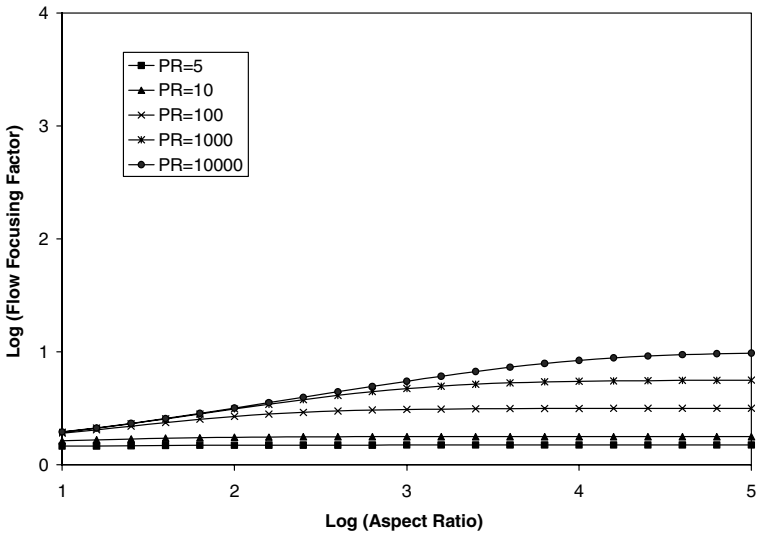


Figure 10. Variation of flow focusing factor with aspect ratio due to different permeability ratios (Inflow parallel to the X axis,  $\theta = 45^\circ$ ).



**Figure 11.** Variation of flow focusing factor with permeability ratio due to different aspect ratios (Inflow parallel to the X axis,  $\theta = 45^\circ$ ).



**Figure 12.** Variation of flow focusing factor with aspect ratio due to different permeability ratios (Inflow parallel to the X axis,  $\theta = 60^\circ$ ).

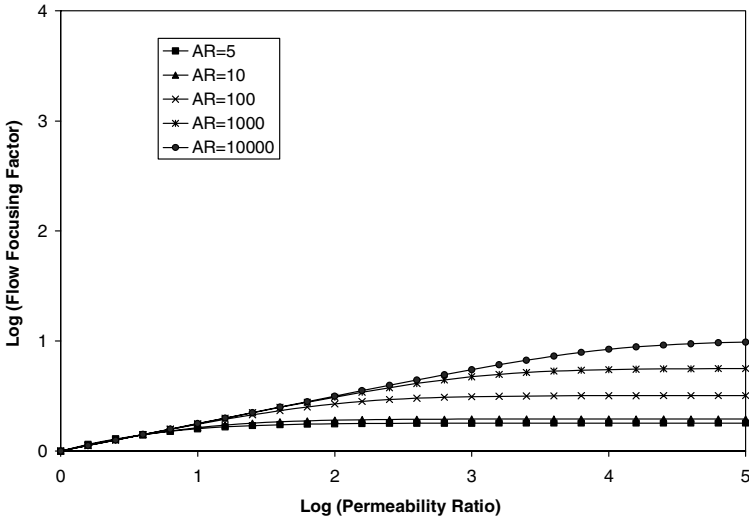


Figure 13. Variation of flow focusing factor with permeability ratio due to different aspect ratios (Inflow parallel to the X axis,  $\theta = 60^\circ$ ).

show the variation of analytical flow focusing factors with the aspect ratio of the inclusion for several different permeability ratios (i.e. PR in these figures) due to the three different dip angles. Figures 9, 11 and 13 show the variation of analytical flow focusing factors with the permeability ratio of the inclusion to its surrounding rock for several different aspect ratios (i.e. AR in these figures) due to the three different dip angles. Clearly, the maximum value of the pore-fluid-flow focusing factor decreases with the increase of the dip angle of the inclusion. With the permeability ratio being 10000 taken as an example, the maximum logarithm value of the pore-fluid-flow focusing factor can reach 2.969 in the case of  $\theta = 30^\circ$ , while it decreases to 1.979 and 0.99 in the case of  $\theta = 45^\circ$  and  $\theta = 60^\circ$  respectively. The previous findings, such as the variation trend of pore-fluid-flow focusing factors with either different permeability ratios or different aspect ratios of the inclusion, can be also observed from the analytical solutions shown in Figures 8–13.

### CONCLUSIONS

Exact analytical solutions have been derived rigorously for the pore-fluid velocity, the pore-fluid flow focusing factor, the stream function and the excess pore-fluid pressure around and within a buried inclined elliptic inclusion with any dip angles. The present analytical solutions provide a useful tool for fundamentally understanding the general behaviour of pore-fluid flow around and within buried faults and large cracks.

The present analytical solution for the pore-fluid-flow focusing factor within a buried inclined inclusion has been used to demonstrate how pore-fluid flow is focused into the buried inclined inclusion. It has been found that the pore-fluid-flow focusing factor of a buried elliptic inclusion is dependent on the aspect ratio, the permeability ratio and the dip angle of the inclusion. Therefore, it can be directly used to investigate the pore-fluid-flow focusing phenomenon within the buried faults and large cracks within the crust of the Earth.

## REFERENCES

- Connolly, J. A. D., 1997, Mid-crustal focused fluid movements: Thermal consequences and silica transport, *in* Jamtveit, B. and Yardley, B. W. D., eds., *Fluid flow and transport in rocks: Mechanics and effects*, Chapman and Hall, London, 319 p.
- Gerhart, P. M., Gross, R. J., and Hochstein, J. I., 1993, *Fundamentals of fluid mechanics*: Addison-Wesley, New York, 983 p.
- Jamtveit, B., and Yardley, B. W. D., 1997, *Fluid flow and transport in rocks: mechanisms and effects*: Chapman and Hall, London, 319 p.
- Lamb, H., 1975, *Hydrodynamics*: Cambridge University Press, London, 738 p.
- Phillips, O. M., 1991, *Flow and reactions in permeable rocks*: Cambridge University Press, Cambridge, 279 p.
- Zhao, C., and Valliappan, S., 1994a, Numerical modelling of transient contaminant migration problems in infinite porous fractured media using finite/infinite element technique: Theory: *Int. J. Num. Anal. Meth. Geomech.*, v. 18, p. 523–541.
- Zhao, C., and Valliappan, S., 1994b, Numerical modelling of transient contaminant migration problems in infinite porous fractured media using finite/infinite element technique: Parametric study: *Int. J. Num. Anal. Meth. Geomech.*, v. 18, p. 543–564.
- Zhao, C., Hobbs, B. E., Mühlhaus, H. B. and Ord, A., 1999, Finite element analysis of flow patterns near geological lenses in hydrodynamic and hydrothermal systems: *Geophys. J. Int.*, v. 138, p. 146–158.
- Zhao, C., Lin, G., Hobbs, B. E., Mühlhaus, H. B., Ord, A., and Wang, Y., 2001, Finite element modelling of heat transfer through permeable cracks in hydrothermal systems with upward throughflow: *Eng. Comput.*, v. 18, p. 996–1011.
- Zhao, C., Hobbs, B. E., Mühlhaus, H. B., Ord, A., and Lin, G., 2002, Analysis of steady-state heat transfer through mid-crustal vertical cracks with upward throughflow in hydrothermal systems: *Int. J. Num. Anal. Meth. Geomech.*, v. 26, p. 1477–1491.